Supplemental Table of Contents

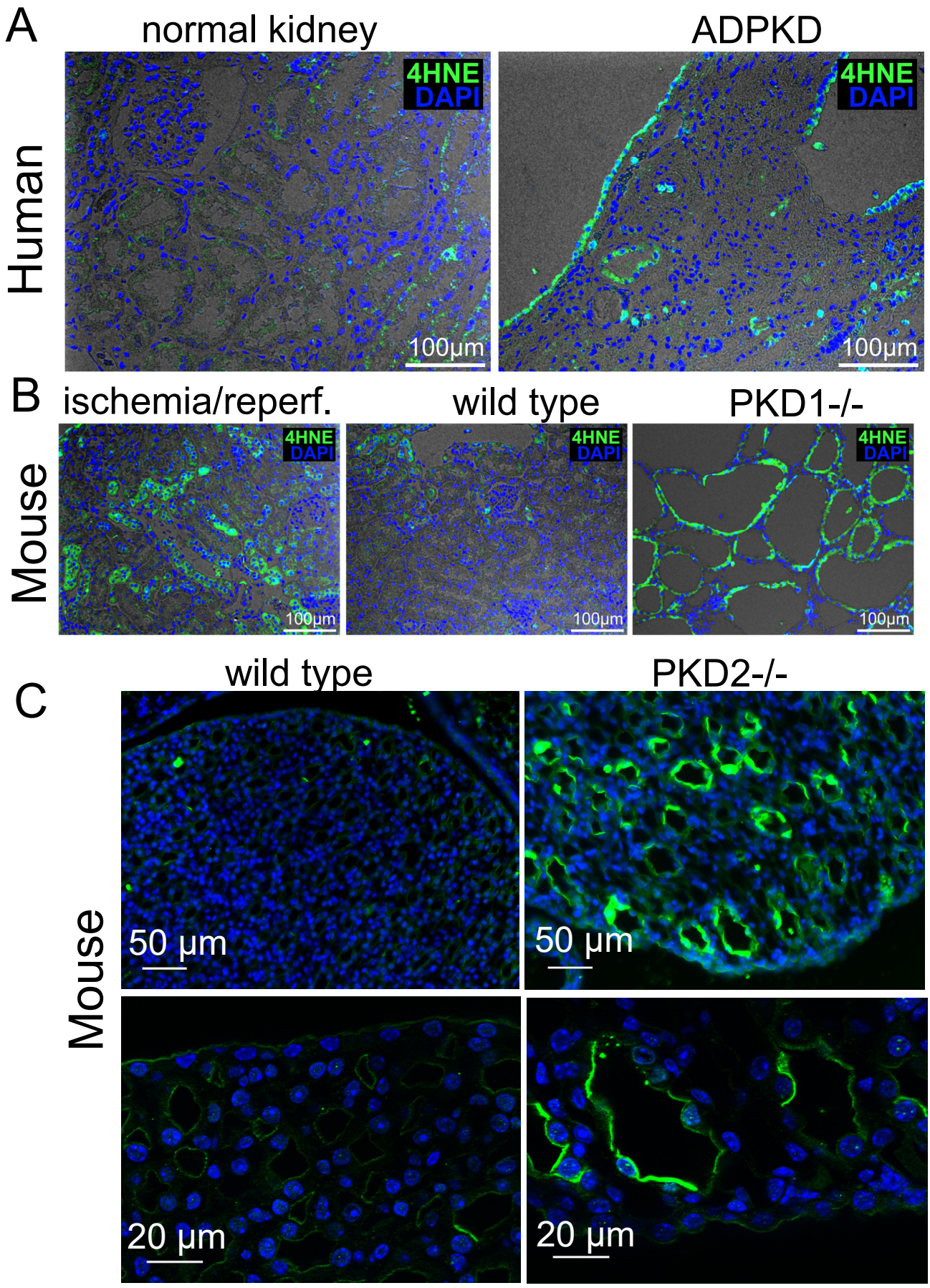

Supplementary Figure 1: *Lipid peroxidation in kidneys from human and mouse ADPKD.* 4-hydroxynonenal (4HNE) staining indicating largely enhanced lipid peroxidation in renal cyst lining epithelium of A) human ADPKD, B) mouse PKD1 knockout and C) mouse PKD2 knockout).

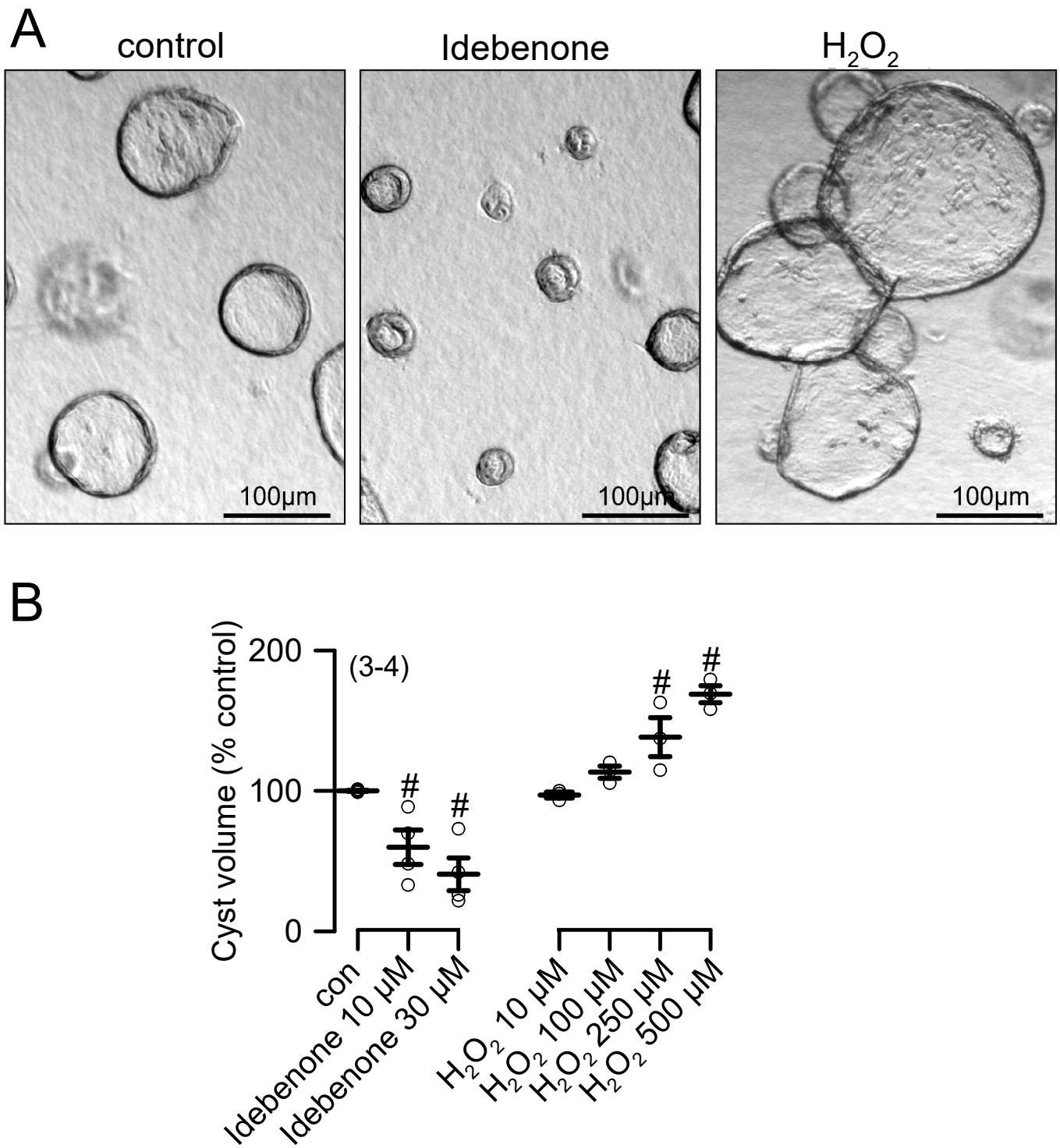

Supplementary Figure 2: *ROS-dependent cyst growth.* A) Growth of MDCK cysts in 3-D matrigel cultures under control conditions (con) or in the presence of different concentrations of the antioxidant compound idebenone or hydrogen peroxide (H_2O_2), respectively. B) Analysis of cyst size relative to the size under control conditions. Mean ± SEM (number of assays). #significantly different when compared to control ($p<0.05$, ANOVA).

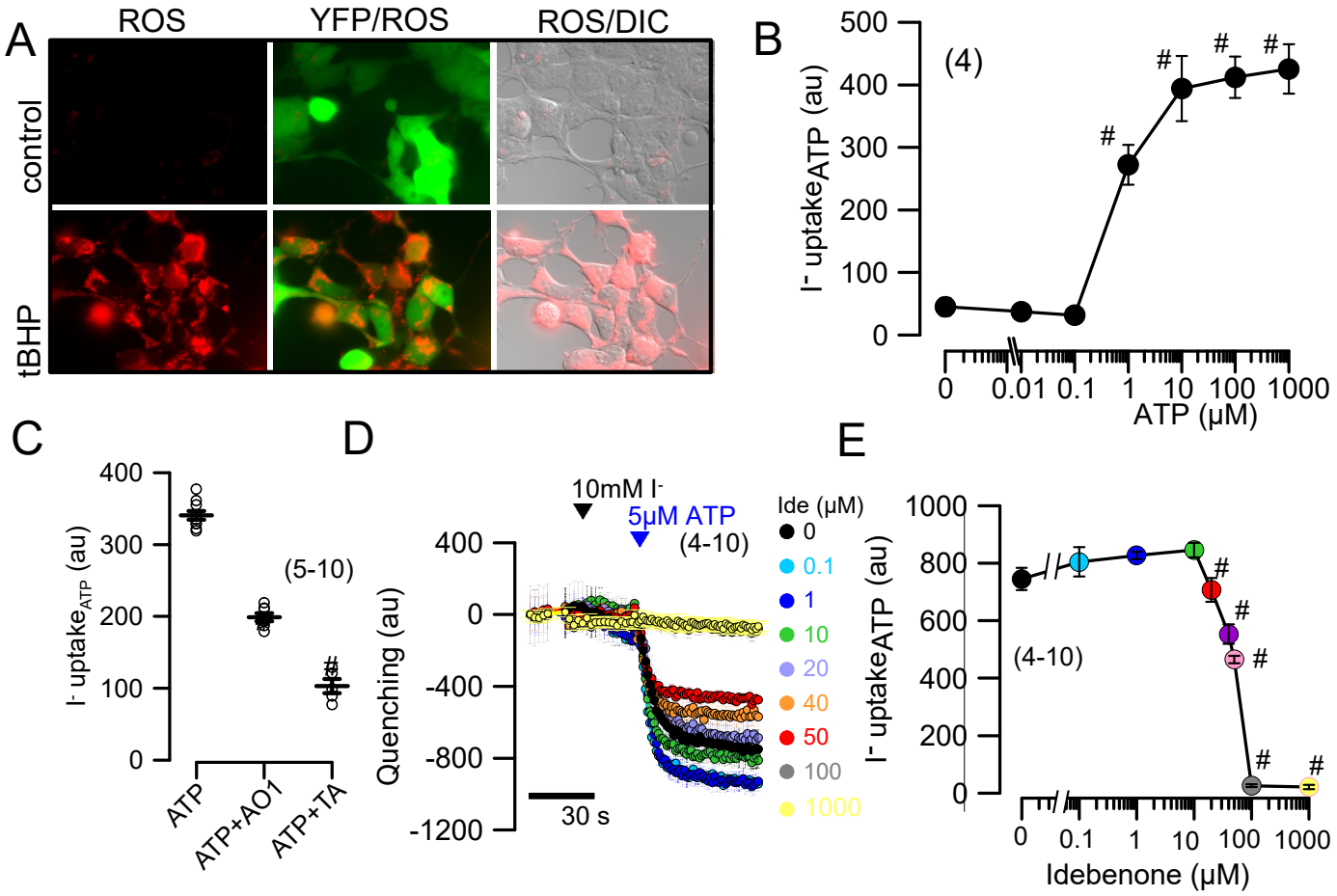

Supplementary Figure 3: *Inhibition of halide conductance by idebenone.* A) Detection of reactive oxygen species (ROS) induced by tert-butyl hydroperoxide (tBHP; 100 μM) using MAK142 fluorescence in HEK293 cells stably expressing YFP and TMEM16A. Green fluorescence, YFP-expression. DIC, differential interference contrast. B) Concentration response for the effect of ATP on YFP-quenching by activation of I^- uptake. C) Summary for the effects of ATP (5 μM) on YFP-quenching and inhibition of quenching by the TMEM16A-blockers CaCCinhAO1 (AO1, 20 μM) and tannic acid (TA, 20 μM). D,E) Inhibition of ATP-induced YFP-quenching by different concentrations of idebenone. In all experiments, idebenone was pre-incubated for 30 min. Mean ± SEM (number of assays). #significantly different when compared to control ($p<0.05$, ANOVA).

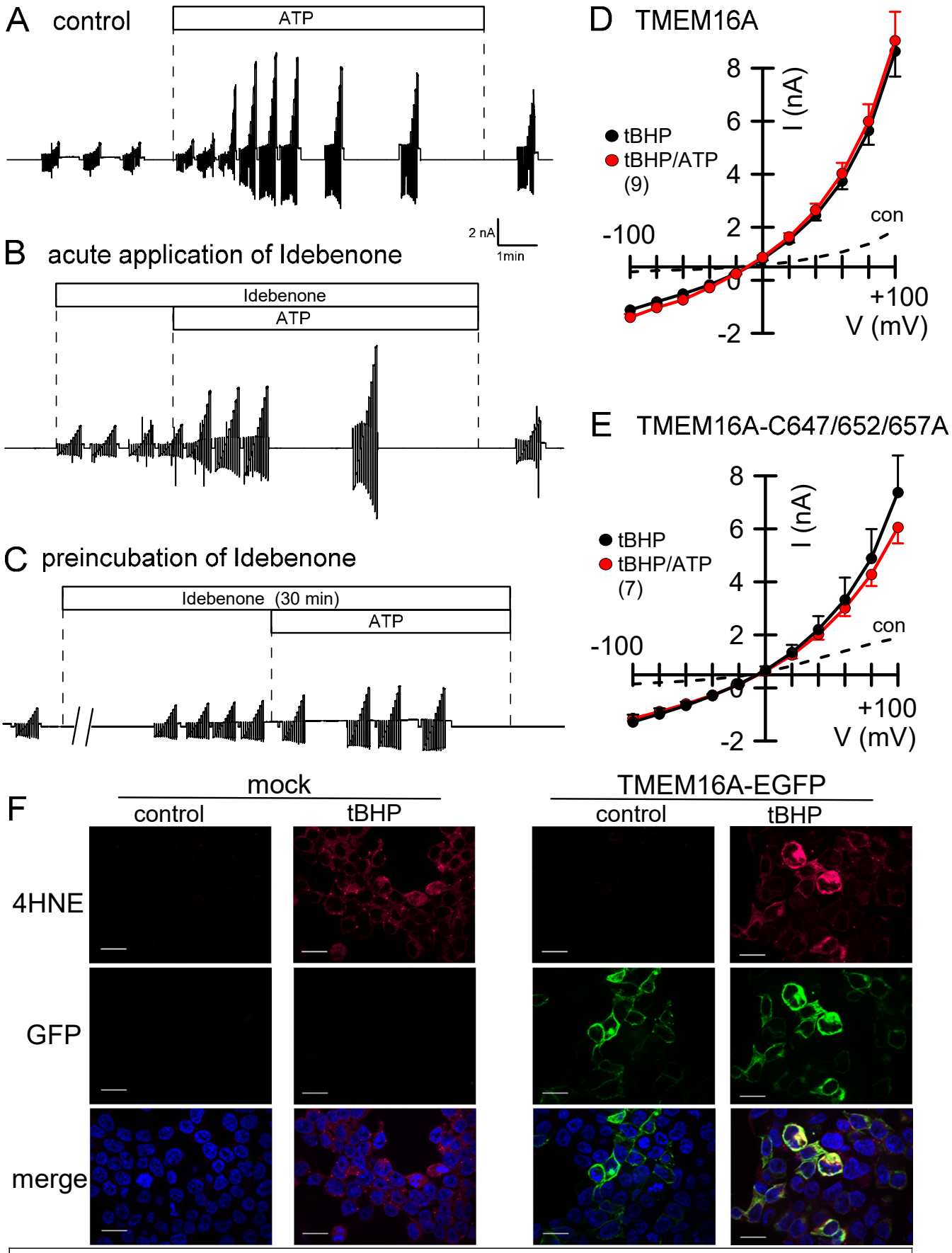

Supplementary Figure 4: *Activation and inhibition of TMEM16A.* A) Continuous whole cell current recordings (clamp voltages ± 100 mV for 1s) showing activation of TMEM16A by purinergic stimulation with ATP (100 µM). B) Activation of TMEM16A by ATP was not inhibited by acute application of idebenone (50 µM). C) Activation of TMEM16A was inhibited by 5 min preincubation of the cell with idebenone. D) TMEM16A activated by tBHP (100 µM) was not further activated by additional stimulation with ATP (100 µM). E) A TMEM16A mutant in which three cysteines in the putative pore-forming domain were replaced by alanines (TMEM16A-C647/652/657A) was still activated by tBHP or tBHP/ATP. F) Lipid peroxidation (4HNE positivity, red) was similar in the absence or presence of TMEM16A-EGFP (green). TMEM16A itself did not activate lipid peroxidation. Bar = 20 µm.

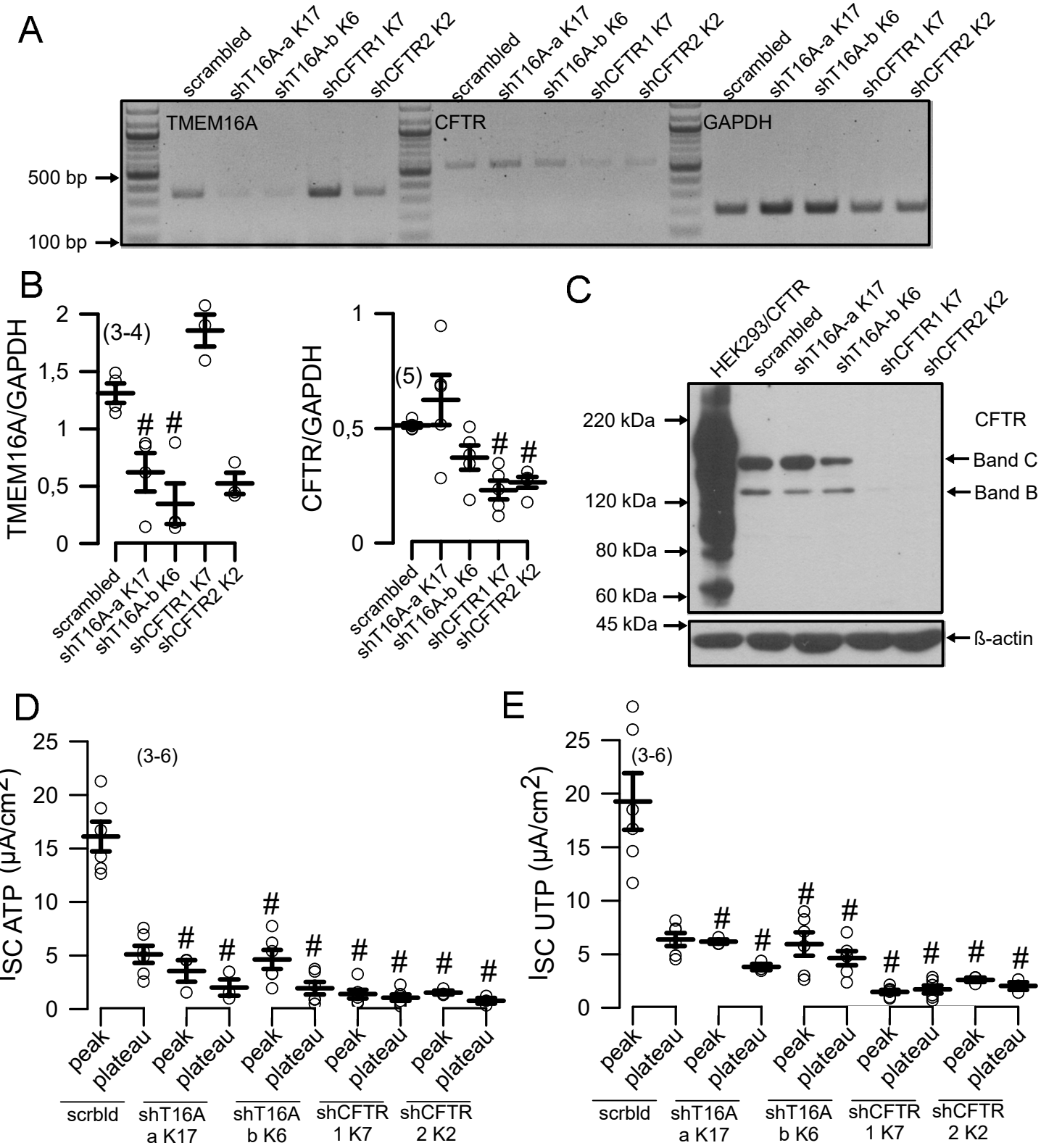

Supplementary Figure 5: *Loss of Cl^- secretion by knockdown of TMEM16A or CFTR.* A) RT-PCR from MDCK clones (MDCK-C7, M/+16A cells) after stable sh-RNA-knockdown of TMEM16A or CFTR, or treatment with scrambled RNA, respectively. B) Analysis from semiquantitative RT-PCR indicating knockdown of TMEM16A (T16A) and CFTR, respectively. C) Western blot of CFTR indicating knockdown by shRNAs. D,E) Summary of short circuit currents assessed in Ussing chamber recordings. Knockdown of both TMEM16A and CFTR eliminated Ca^{2+} activated Cl^- secretion induced by stimulation with ATP or UTP (both 100 µM). Mean ± SEM (number of experiments). #significant difference from scrambled (ANOVA).